

“The equatorial funneling effect”

1982 review paper on “Geostrophic Turbulence”

Lectures at the International School of Physics

Enrico Fermi

7-19 July, 1980

Mini-course on geostrophic turbulence

The Idea:

The same arguments by which we convince ourselves that the energy in two-dimensional turbulence moves to larger scales also predict:

1. Mesoscale energy in the ocean moves toward the equator and into barotropic mode.
2. At the equator, the energy is equipartitioned among vertical modes.

This explains the "deep equatorial jets."



Villa Montesaro



View of Lake Como

Two-dimensional turbulence

$$\frac{\partial}{\partial t} \nabla^2 \psi + J(\psi, \nabla^2 \psi) = 0$$

Conserves:

$$\text{Energy} = \frac{1}{2} \iint d\mathbf{x} \nabla \psi \cdot \nabla \psi = \int_0^\infty dk E(k)$$

$$\text{Enstrophy} = \frac{1}{2} \iint d\mathbf{x} (\nabla^2 \psi)^2 = \int_0^\infty dk k^2 E(k)$$

Energy moves to smaller k . Enstrophy moves to larger k .

Two-layer QG turbulence

$$\frac{\partial q_i}{\partial t} + J(\psi_i, q_i) = 0$$

$$\text{top layer } q_1 = \nabla^2 \psi_1 + \frac{1}{2} k_R^2 (\psi_2 - \psi_1) + \beta y$$

$$\text{bottom layer } q_2 = \nabla^2 \psi_2 + \frac{1}{2} k_R^2 (\psi_1 - \psi_2) + \beta y, \quad k_R^2 \equiv \frac{2f_0^2}{g'H}$$

Simplifying assumptions:

1. Equal mean layer depths H
2. Flat bottom, rigid lid
3. Channel geometry

Conserves:

$$\text{Energy} = \frac{1}{2} \iint d\mathbf{x} \left(\nabla \psi_1 \cdot \nabla \psi_1 + \nabla \psi_2 \cdot \nabla \psi_2 + \frac{1}{2} k_R^2 (\psi_1 - \psi_2)^2 \right)$$

$$\text{Potential enstrophies} = \frac{1}{2} \iint d\mathbf{x} q_i^2 \quad \text{assumed equal (for simplicity)}$$

Introduce vertical modes:

$$\begin{bmatrix} \psi_1(x,y,t) \\ \psi_2(x,y,t) \end{bmatrix} = \psi(x,y,t) \begin{bmatrix} 1 \\ 1 \end{bmatrix} + \tau(x,y,t) \begin{bmatrix} 1 \\ -1 \end{bmatrix}$$

then :

$$\text{Energy: } \iint d\mathbf{x} (\nabla \psi \cdot \nabla \psi + \nabla \tau \cdot \nabla \tau + k_R^2 \tau^2) = \int dk (U(k) + T(k))$$

$$\text{Potential Enstrophy: } \iint d\mathbf{x} ((\nabla^2 \psi)^2 + (\nabla^2 \tau - k_R^2 \tau)^2) = \int dk (k^2 U(k) + (k^2 + k_R^2) T(k))$$

The conservation laws take the same form as in 2DT, but:

The barotropic modes have a wavenumber (squared) of k^2

The baroclinic modes have an effective wavenumber (squared) of $k^2 + k_R^2$

This puts the baroclinic modes at a disadvantage:

At horizontal scales larger than the deformation radius,
energy should concentrate in barotropic mode.

M vertical modes (or layers):

$\psi_0(x, y, t)$ (formerly ψ) barotropic mode (no zero crossings)

$\psi_1(x, y, t)$ (formerly τ) first baroclinic mode (1 zero crossing)

\vdots

$\psi_n(x, y, t)$ n th baroclinic mode (n zero crossings)

$$\text{Energy} = \int dk \left(E_0(k) + E_1(k) + E_2(k) + \dots \right)$$

$$\text{Potential Enstrophy} = \int dk \left(k^2 E_0(k) + (k^2 + k_1^2) E_1(k) + (k^2 + k_2^2) E_2(k) + \dots \right)$$

$$k_n \equiv \frac{n\pi f_0}{NH}, \quad H = \text{total depth}, \quad N = \text{Vaisala frequency (assumed uniform)}$$

The higher baroclinic modes are even more brutally penalized than the first baroclinic mode.

At midlatitudes, all energy eventually becomes barotropic.

M The most convincing argument for this involves equilibrium statistical mechanics:

For 2DT (Kraichnan, 1967),
$$E(k) = \frac{k}{\alpha + \gamma k^2}$$

For 2LT,
$$U(k) = \frac{k}{\alpha + \gamma k^2}, \quad T(k) = \frac{k}{\alpha + \gamma(k^2 + k_R^2)}$$

For *M* vertical modes,
$$E_n(k) = \frac{k}{\alpha + \gamma \left(k^2 + \frac{n^2 \pi^2 f_0^2}{N^2 H^2} \right)}$$

Suppose that we replace $f \rightarrow \beta y$

Then
$$E_n(k, y) = \frac{k}{\alpha + \gamma \left(k^2 + \frac{n^2 \pi^2 \beta^2 y^2}{N^2 H^2} \right)}$$
 For $n > 0$, $E_n(k)$ increases toward the equator.

What happens at $y = 0$?

There is an equatorial peak in $E_n(k, y)$.

The width of the peak is obtained by equating k^2 and $\frac{n^2 \pi^2 \beta^2 y^2}{N^2 H^2}$ with $k \sim \frac{1}{y}$

That is, the equatorial peak in $E_n(k, y)$ has a width equal to the n -th deformation radius.

$\psi_n(x, y, t)$ in a 6-layer QG equatorial channel

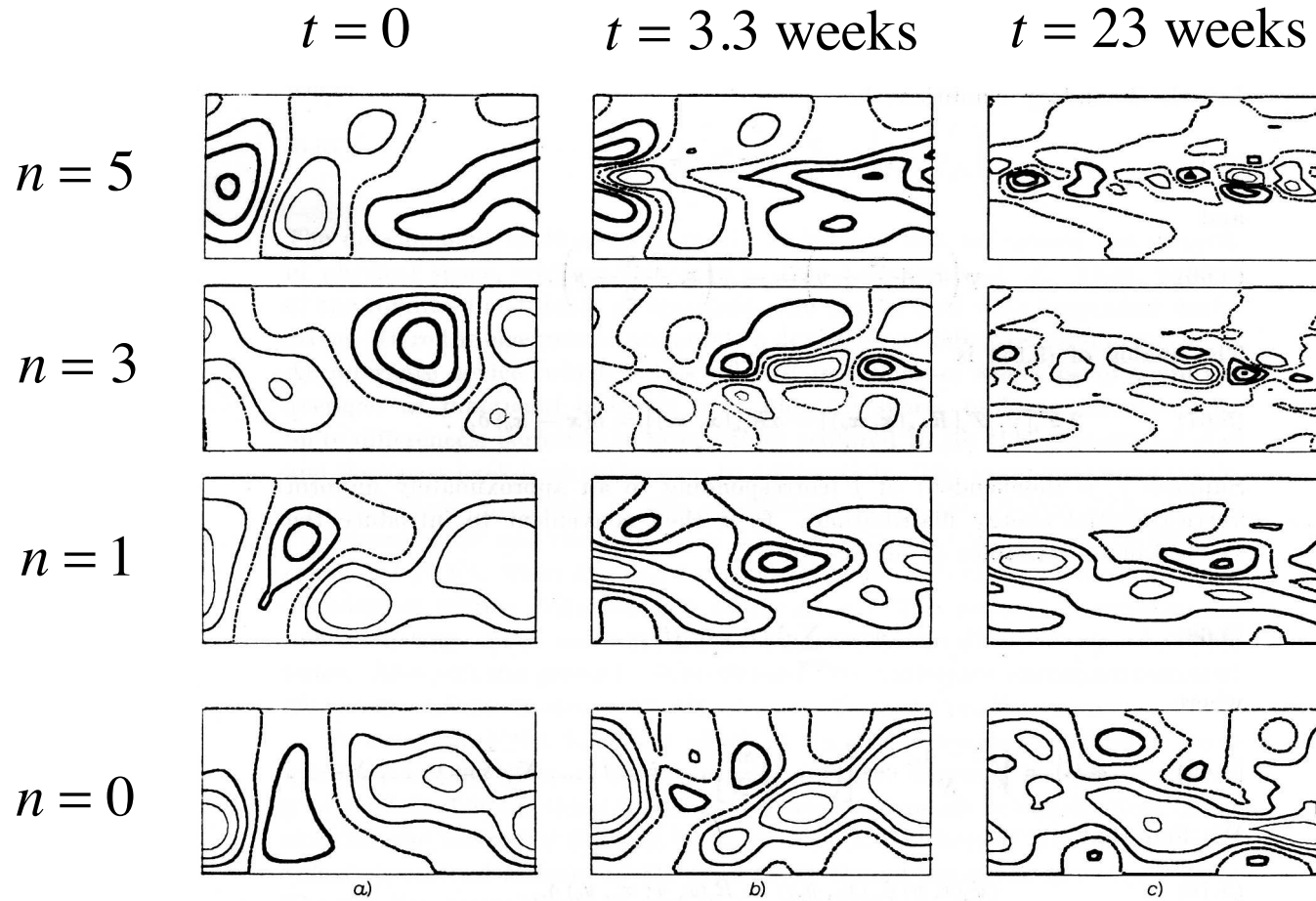


Fig. 7. - The vertical-mode streamfunctions ψ_s in the equatorial channel ($0 < x < 2\pi$, $-\pi/2 < y < \pi/2$) for the barotropic mode $s = 0$ (bottom), $s = 1$, $s = 3$ and $s = 5$ (top). The equator lies along the axis of the channel. a) weeks = 0, b) weeks = 3.346, c) weeks = 23.421.

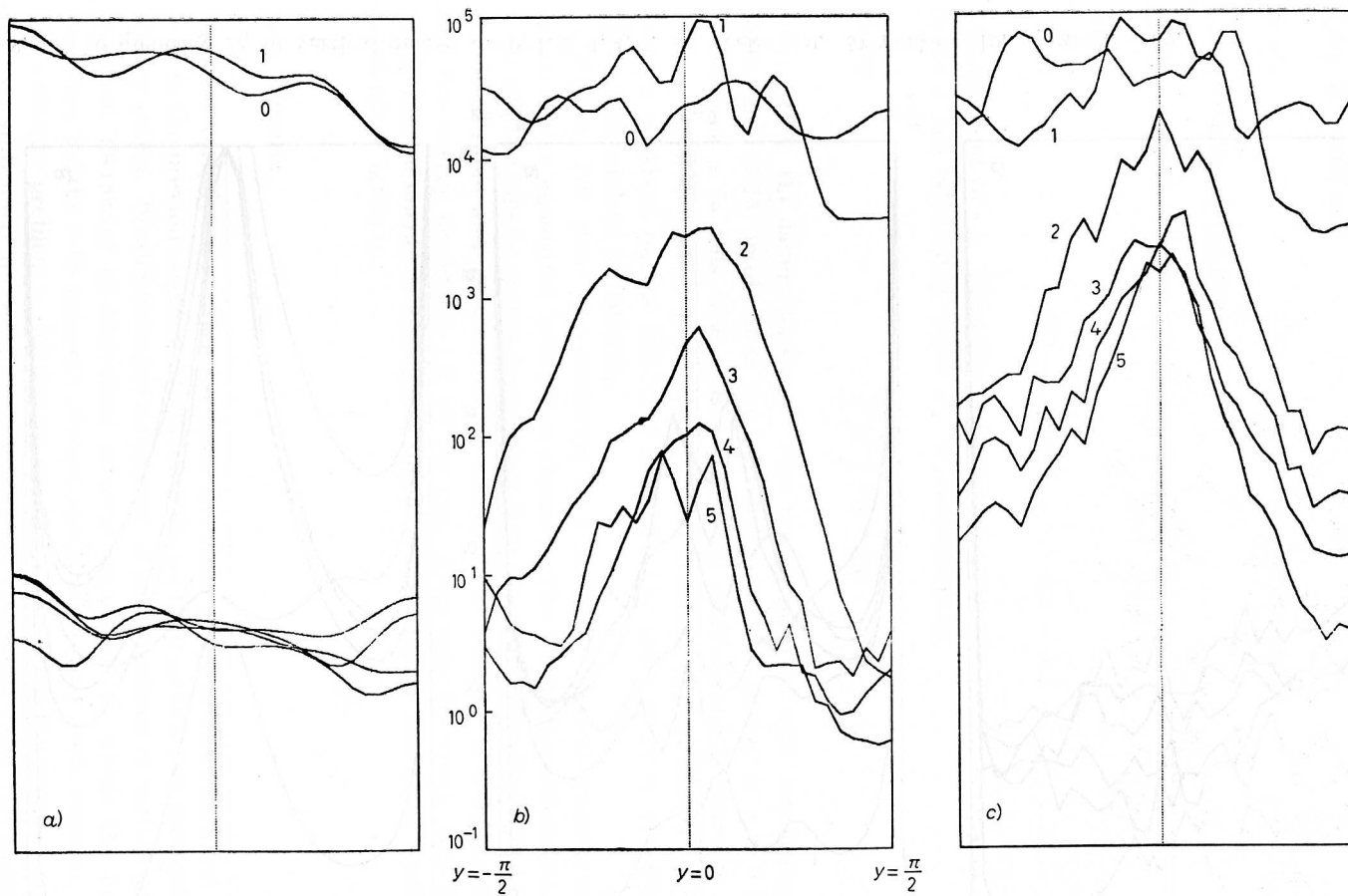


Fig. 8. - The kinetic energy averaged over x in the vertical modes $s = 0, 1, 2, 3, 4, 5$. The equator lies at $y = 0$. a) weeks = 0, b) weeks = 10, c) weeks = 30.

Luyten & Swallow (1976)

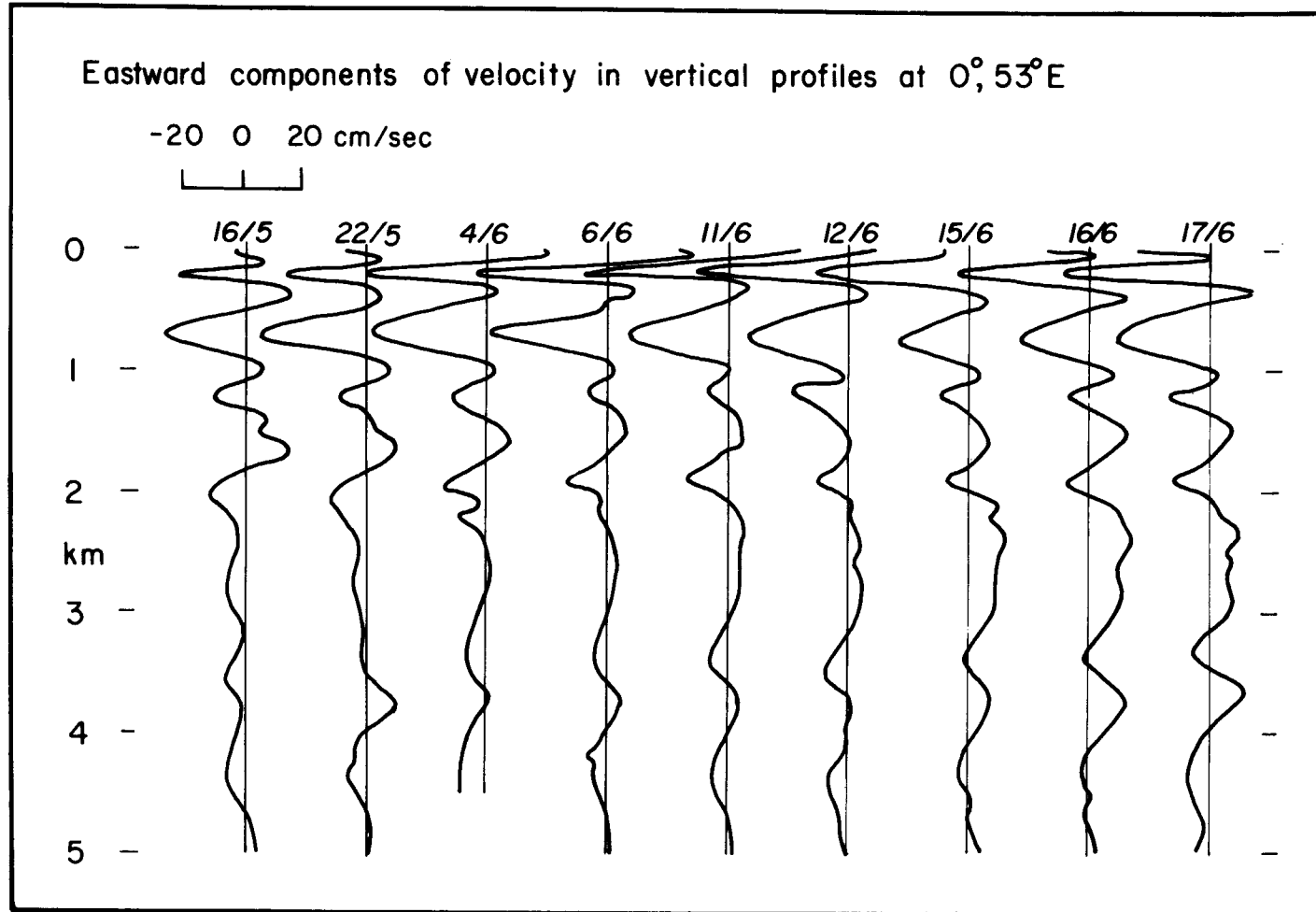


Figure 1

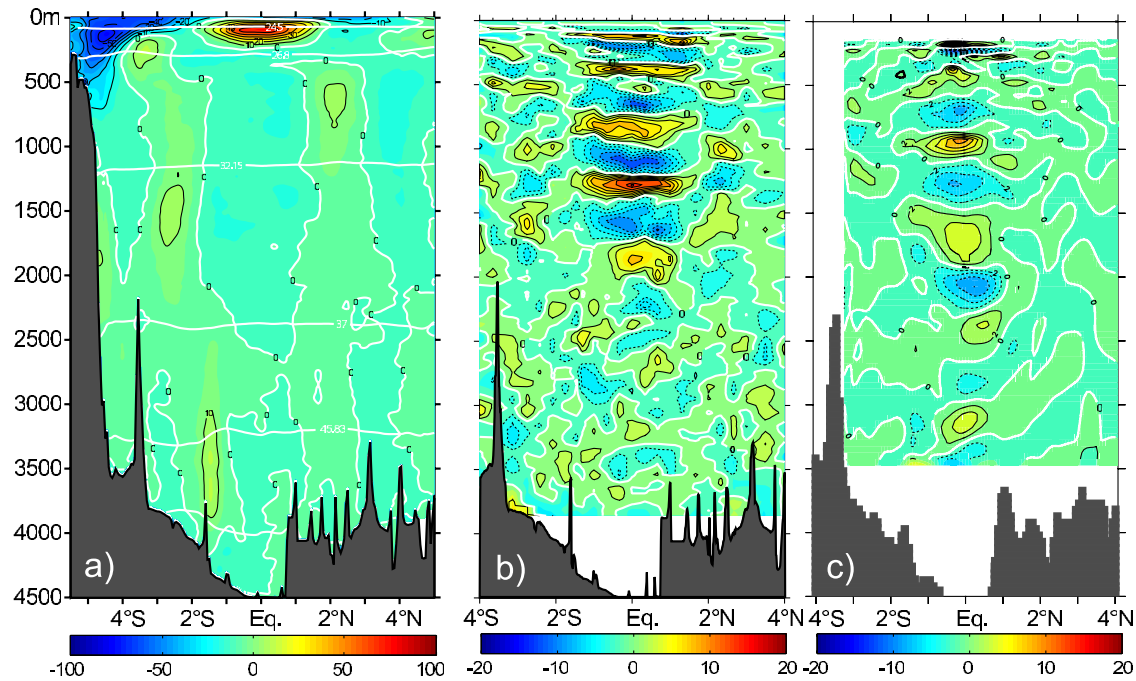


Figure 1. (a) Mean zonal flow at 35°W determined from 16 repeat sections. Color contours change every 5 cm s⁻¹ while black contour lines indicate changes in velocities of 10 cm s⁻¹. (b) Instantaneous zonal velocity section as observed in May 2003 from which the zonal flow of the first nine vertical modes has been removed. Stations spacing was 1/3° within 2° of the equator and 1/2° elsewhere. Color contour interval is 2 cm/s, while black lines separate velocities increased by 5 cm/s. Data from depths below 3850 m are not displayed. (c) Instantaneous zonal velocity from which the first nine vertical modes has been removed in a model simulation (experiment 1/12–94). Contour interval is identical to Figure 1b.

Two-layer Turbulence

64 x 64 gridpoints, $H_1 / H_2 = 1 / 7$, $U_1 / U_2 = 4 / 1$

Initially uncorrelated streamfunctions

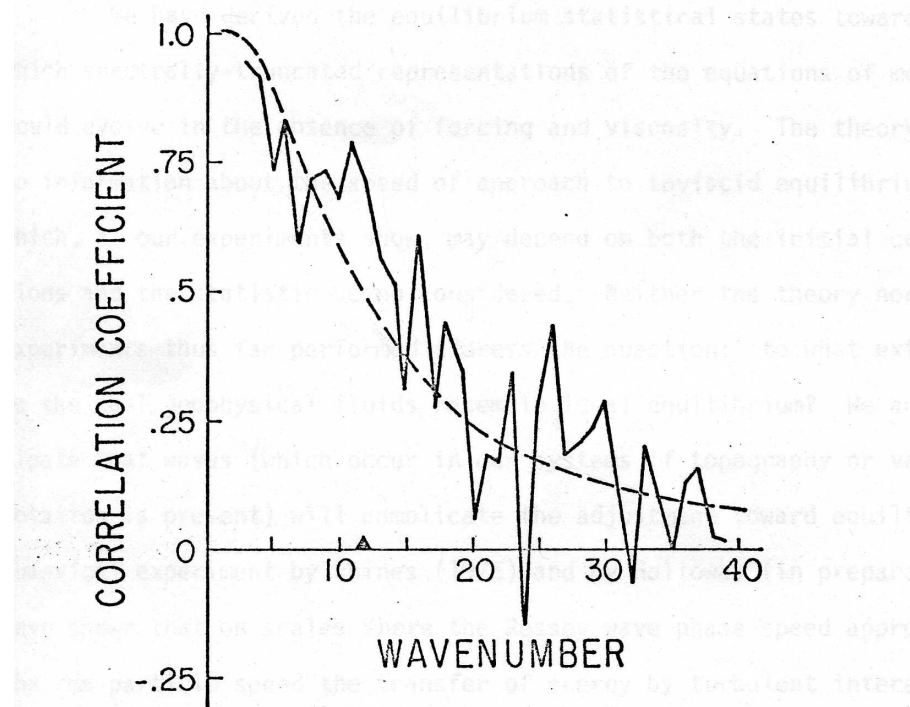


Figure 2.5b The correlation between layers in experiment B after 498 days (solid curve) and the theoretical equilibrium correlation (dashed curve).